ISSN 1392-1207. MECHANIKA. Vol. 30, No. 3, 2024: 251–259

Active Control for Transverse Vibration of the Marine Stern Shaft-Bearing System with LQR Strategy

Qianwen HUANG*, Qingnan HU, Huaiguang LIU*****
**Hubei Key Laboratory of Mechanical Transmission and Manufacturing Engineering, School of Machinery and Automation, Wuhan University of Science and Technology, Wuhan, 430081, China, E-mail: qwhuang@wust.edu.cn*
***School of Machinery and Automation, Wuhan University of Science and Technology, Wuhan, 430081, China, E-mail: 1026538689@qq.com*
****Hubei Key Laboratory of Mechanical Transmission and Manufacturing Engineering, School of Machinery and Automation, Wuhan University of Science and Technology, Wuhan, 430081, China, E-mail: liuhuaiguang@wust.edu.cn*
https://doi.org/10.5755/j02.mech.35373

1. Introduction

The marine stern shaft-bearing systems are the important part of the power transmission for the ships as it delivers torque to propel the ship's motion [1]. The most significant vibration form is the transverse vibration [2], which becomes further complicated due to the effect of main engine, propeller and the lubrication bearings [3]. It is undesired that the vibration of the shaft will be enhanced and the wear of the bearing may be enlarged [4, 5]. Therefore, the vibration reduction of the marine shaft-bearing systems is significant for the improvement of service life and transfer efficiency [6, 7].

The first familiar control method for the vibration suppression is passive control method [8]. It is widely applied as the main control principle is to modify structural parameters or add vibration absorption to the system [9]. While, the reduction of stiffness and variation of damping will be caused, which leads to the applicable frequency ranges is limited [10]. The controlled behaviors between low and high frequency are much discrepant due to the variable damping [11]. Another usual approach of the vibration reduction is semi-active control [12]. It is a parametric control process that relies on structural response and external excitation of the system [7]. The actuator that provides the control force only needs a small amount of energy to enable it to achieve the optimal value based on the reciprocal relative motion of the system [13]. But it poses a relative difficulty in the design of semi-active systems and can only realize the control force related to speed. The third commonly strategy to reduce undesirable vibration generated by the system is active control [14]. It is designed with an appropriate force or moment actuator to resist the vibration in its direction [15]. The active control can be used for a wider frequency range than passive control in many engineering applications [16]. However, some of the active strategies may induced chattering effect or instability to the system.

As the high control efficiency of the active control, the researches regarding to the marine shaft-bearing system have been widely investigated. H. Zheng et al. [17] studied the active control for longitudinal vibration of the propeller shaft through dynamic interpolation method with control force applied to the thrust bearing. X. Xie et al. [18] designed an adaptive control algorithm with active stern support for the vibration reduction that from the propeller shaft to the hull structures. N. Duan et al. [19] analyzed the active control on the power source with a control target of acceleration for attenuation of the transvers vibration transmission. Although a large number of studies have been carried out, there still exists problem to be solved.

As the vibration control has inevitable influence on the transmission reliability of the propulsion system, the choice of the control strategy should be more efficiency and accuracy [20]. The reasonable structural design of the controlled system and the simplification of the dynamical model had significant influence on the vibration reduction [21]. The accurate definition and the adjustability of the control parameters are important parts [22]. There will be differences between the controlled model and the actual system, and it is hard to realize expected controlled behavior.

Given this, the active vibration control of the marine stern shaft-bearing systems is investigated on the basis of LQR strategy. The controlled behaviors and robustness analysis are calculated and then compared to that of the passive control. The effect of damping absorber is explored through results discussion with different damping coefficient. The setting time, overshoot rate and reduction rate have also been analyzed with different control weighting matrix. Therefore, the vibration reduction of the marine stern shaft-bearing systems can be achieved with the proposed LQR strategy.

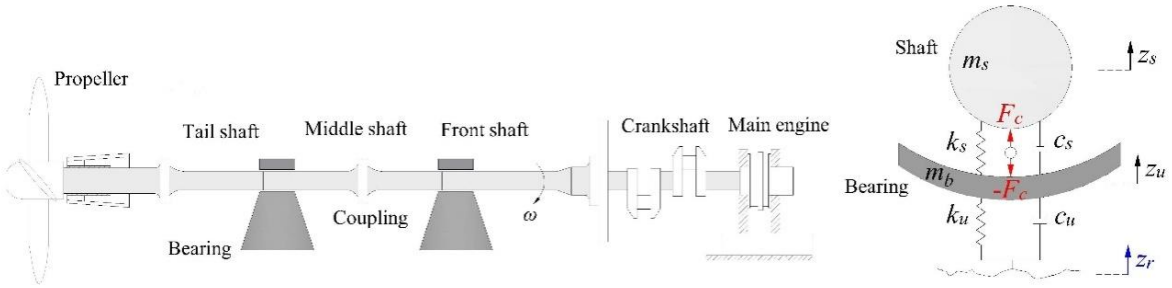

Fig. 1 Schematic of the marine stern shaft-bearing system and the control system

2. Methodology

2.1. Dynamical model of the system

The schematic of Fig. 1 represents the marine stern shaft-bearing system with the controlled system is installed closed to the tail shaft. The designed controller consists of an adjustable damping vibration absorber and an electromagnetic force actuator. The force F_c generated by the actuator is a combination of changeable damping force and electromagnetic force. The shock absorber is simplified as dampers and is placed between the clearance of the shaft and the bearing. Here, z_r is the disturbance input on the stern bearing.

Considering the generated force from the actuator of the controlled system, the motion equation of the marine stern shaft-bearing systems can be given on the basis of Newton's second law:

$$\begin{aligned} m_s\ddot{z}_s &= -c_s\left(\dot{z}_s-\dot{z}_u\right)-k_s\left(z_s-z_u\right)+F_c,\\ m_u\ddot{z}_u &= -c_u\left(\dot{z}_u-\dot{z}_r\right)-c_s\left(\dot{z}_u-\dot{z}_s\right)-k_u\left(z_u-z_r\right)-k_s\left(z_u-z_s\right)-F_c, \end{aligned} \tag{1}$$

where m_s, c_s, and k_s are the mass, equivalent damping and stiffness (dampers and springs of the controller) of the sprung shaft, respectively. And the m_u, c_u, and k_u represent the mass, inherent damping and stiffness of the bearing. The F_c is the force of the actuator. The displacement, velocity and acceleration of the sprung shaft are z_s, $\dot{z}_s$ and $\ddot{z}_s$ respectively. And that of the corresponding unsprung bearing are defined as z_u, $\dot{z}_u$ and $\ddot{z}_u$.

After converting the acceleration of the shaft and the bearing, the motion equation can be rewritten as:

$$\begin{aligned} \ddot{z}_s &= \frac{-c_s}{m_s}\left(\dot{z}_s-\dot{z}_u\right)-\frac{k_s}{m_s}\left(z_s-z_u\right)+\frac{F_c}{m_s},\\ \ddot{z}_u &= -\frac{c_u}{m_u}\left(\dot{z}_u-\dot{z}_r\right)-\frac{c_s}{m_u}\left(\dot{z}_u-\dot{z}_s\right)-\frac{k_u}{m_u}\left(z_u-z_r\right)-\frac{k_s}{m_u}\left(z_u-z_s\right)-\frac{F_c}{m_u}. \end{aligned} \tag{2}$$

2.2. State space representation

The state space equation of the dynamic system can be expressed as:

$$\begin{aligned} \dot{\boldsymbol{x}} &= \boldsymbol{A}\boldsymbol{x}+\boldsymbol{B}\boldsymbol{u},\\ \boldsymbol{y} &= \boldsymbol{C}\boldsymbol{x}+\boldsymbol{D}\boldsymbol{u}, \end{aligned} \tag{3}$$

where $\boldsymbol{x}$, $\boldsymbol{u}$ and $\boldsymbol{y}$ are the vectors of state variables, inputs and outputs, respectively. Combining the dynamical model in Eq. (2) and the state space equation in Eq. (3), the values of $\boldsymbol{x}$, $\boldsymbol{u}$ and $\boldsymbol{y}$ can be defined for the elimination of quadratic high order terms:

$$\boldsymbol{x}=\begin{bmatrix} x_1\\ x_2\\ x_3\\ x_4 \end{bmatrix}=\begin{bmatrix} z_s-z_u\\ \dot{z}_s\\ z_u-z_r\\ \dot{z}_u \end{bmatrix},\ \boldsymbol{u}=\begin{bmatrix} \dot{z}_r\\ F_c \end{bmatrix},\ \boldsymbol{y}=\begin{bmatrix} z_s-z_u\\ \ddot{z}_s \end{bmatrix}, \tag{4}$$

where $z_s - z_u$ is the suspension travel and $z_u - z_r$ is the soleplate deflection, $\dot{z}_r$ is the velocity of the disturbance input.

The $\boldsymbol{A}$, $\boldsymbol{B}$, $\boldsymbol{C}$ and $\boldsymbol{D}$ are the matrixes of systems, inputs, outputs and feedforward, respectively. According to the structural parameters of the system, the values are defined as:

$$\boldsymbol{A}=\begin{bmatrix} 0 & 1 & 0 & -1\\ -\frac{k_s}{m_s} & -\frac{c_s}{m_s} & 0 & \frac{c_s}{m_s}\\ 0 & 0 & 0 & 1\\ \frac{k_s}{m_u} & \frac{c_s}{m_u} & -\frac{k_u}{m_u} & -\frac{c_s+c_u}{m_u} \end{bmatrix},\ \boldsymbol{B}=\begin{bmatrix} 0 & 0\\ 0 & \frac{1}{m_s}\\ -1 & 0\\ \frac{c_u}{m_u} & -\frac{1}{m_u} \end{bmatrix},\ \boldsymbol{C}=\begin{bmatrix} 1 & 0 & 0 & 0\\ -\frac{k_s}{m_s} & -\frac{c_s}{m_s} & 0 & \frac{c_s}{m_s} \end{bmatrix},\ \boldsymbol{D}=\begin{bmatrix} 0 & 0\\ 0 & \frac{1}{m_s} \end{bmatrix}. \tag{5}$$

2.3. State feedback control

The full-state feedback controller has optimal solution for desired pole position in closed-loop system due to the state variables is known for feedback. The state space matrix $\boldsymbol{x}$ can feed every variable back to the control inputs $\boldsymbol{u}$ through the gain of feedback vector $\boldsymbol{K}$, which is adjustable for desired pole value. The system inputs can be rewritten as:

$$\boldsymbol{u} = -\boldsymbol{K}\boldsymbol{x}, \tag{6}$$

where $\boldsymbol{K}$ is the gain of feedback vector.

The state feedback control for closed-loop system can be obtained by introducing above equation into Eq. (3):

$$\begin{aligned} \dot{\boldsymbol{x}} &= \left(\boldsymbol{A}-\boldsymbol{B}\boldsymbol{K}\right)x,\\ \boldsymbol{y} &= \left(\boldsymbol{C}-\boldsymbol{D}\boldsymbol{K}\right)x. \end{aligned} \tag{7}$$

For controllable system, the controllability matrix should be full rank and is equal to the number of state variables of the system:

$$\begin{aligned} \boldsymbol{Co} &= \left[\boldsymbol{B}\quad \boldsymbol{A}\boldsymbol{B}\quad \boldsymbol{A}^2\boldsymbol{B}\quad \cdots\quad \boldsymbol{A}^{n-1}\boldsymbol{B}\right],\\ Rank\left(\boldsymbol{Co}\right) &= n. \end{aligned} \tag{8}$$

where, $\boldsymbol{Co}$ is the controllability matrix, n is the numbers of state variables. The LQR controller is implemented to the system with the matrices are determined to be controllable.

2.4. Linear Quadratic Regulator

The LQR control is a popular kind of state feedback control as the control parameters will be weighted on the basis of individual desired outcomes. The primary function is to minimize the cost function J through the calculation of optimal gain $\boldsymbol{K}$ according to the weighted sum of various states. The cost function can be given as:

$$J = min\frac{1}{2}\int_0^t \left(x^T \boldsymbol{Q}x + u^T \boldsymbol{R}u + 2x^T \boldsymbol{N}u\right)dt\,, \tag{9}$$

where, x and u are state variables vector and control input vector. The error weighting matrix $\boldsymbol{Q}$ is diagonal positive definite form and the control weighting matrix $\boldsymbol{R}$ is a positive constant. The desired performance will be obtained until suitable results regarding the performance index J reached by values adjusting of the matrices.

Assuming that the Riccati equation can obtain a positive definite symmetric matrix, then the LQR problem has a solution with negative feedback gain:

$$\boldsymbol{K} = R^{-1}\left(\boldsymbol{B}^T\boldsymbol{P} + \boldsymbol{N}\right), \tag{10}$$

where $\boldsymbol{P}$ satisfies the Riccati equation:

$$\boldsymbol{A}^T + \boldsymbol{P}\boldsymbol{A} + \boldsymbol{Q} - \boldsymbol{P}\boldsymbol{B}\boldsymbol{R}^{-1}\boldsymbol{B}^T\boldsymbol{P} = 0\,. \tag{11}$$

Based on Eq. (6), the feedback regulator and solution to the performance index can be given by:

$$F_c = -\boldsymbol{K}\boldsymbol{u}\,. \tag{12}$$

3. Design of active controller

3.1. Active control systems

The abovementioned theoretical models and control methods will be applied into the active LQR control system through Matlab/Simulink with the definition of control parameters. The block diagrams in Fig. 2 displays the structures of both the active and passive control systems. Both the two systems consist of the models of the control system and the functions of subsystems. The models include the dynamical model, state feedback and state-space model.

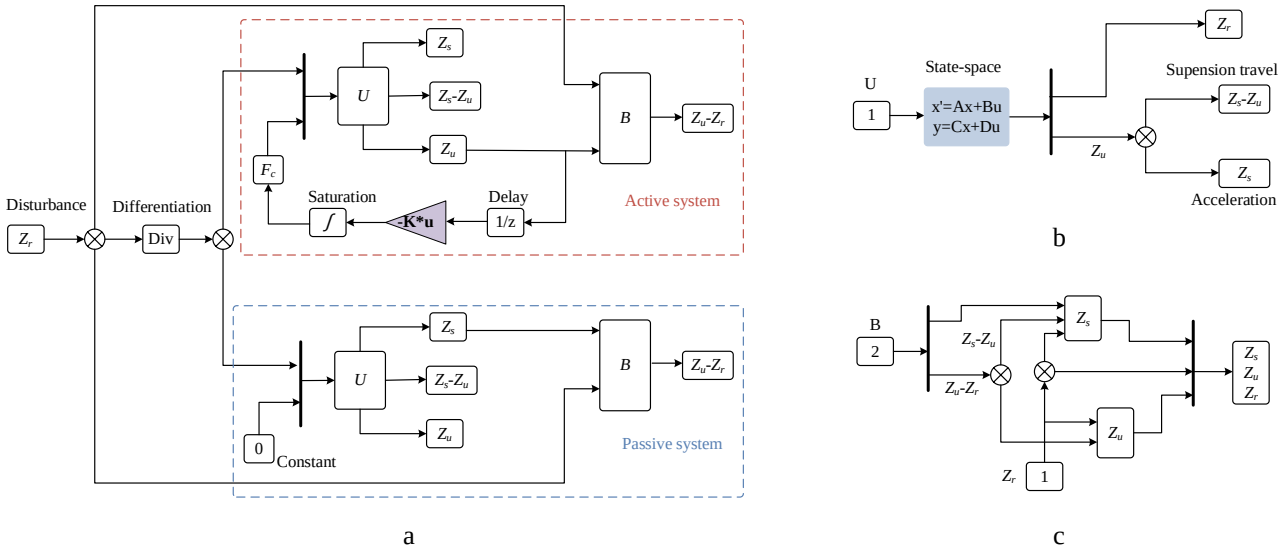

Fig. 2 Structure of the control system: a – structure of the controller, b – state-space model, c – calculation subsystem

It should be pointed out that the discrepancy of the active and passive control system is the electromagnetic actuator. The actuator is only used for active systems and does not take into account in the passive systems. It will generate force to stabilize the system as the state variables are feedbacked to control input $\boldsymbol{u}$ through gain $\boldsymbol{K}$. The disturbance input is followed by a first order filter with transfer function to convert potential sharp step perturbations into smooth edge. The filter is followed by a derivative block for the velocity form of the disturbance input.

In order to implement the behavior of the state variables in Eq. (4), a state-space block U shown in Fig. 2, b is arranged to model the open-loop plant for the analysis of the acceleration of the shaft and the bearing. This state-space model is a subsystem in both the active and passive control systems, respectively. Similarly, a subsystem B displayed in Fig. 2, c is applied to calculate the suspension travel and soleplate deflection. The results for both the active and passive system are calculated.

The results of state variables calculated by the Simulink model will be inputted into the workspace through the workspace block. These workspace blocks will write signal data into the module of MATLAB. The simulation time is defined as 10 sec with an initial value of 0 is selected.

3.2. Definition of control parameters

For the calculation of above-mentioned LQR and passive control system, the control parameters of the calculation are selected to follow the structures of the shaft experimental platform, which are listed in Table 1 [23].

Table 1
The model parameters for numerical simulations

Parameters	Values
Shaft mass m_s	1280 kg
Bearing mass m_u	260 kg
Shaft stiffness k_s	1.7×10^5 N/m
Bearing stiffness k_u	4.6×10^5 N/m
Shaft damping c_s	2.68×10^3 N·s/m
Bearing damping c_u	4.62×10^3 N·s/m

After attempts to verify non-zero elements in the error weighting matrix $\boldsymbol{Q}$ and the control weighting matrix R, the final definition is:

$$\boldsymbol{Q}=\begin{bmatrix}1.76\times10^9 & & & \\ & 1.16\times10^7 & & \\ & & 1 & \\ & & & 1\end{bmatrix},\ R=0.01. \qquad (13)$$

With the definition of $\boldsymbol{Q}$ and R, the matrix $\boldsymbol{P}$ associated with gain $\boldsymbol{K}$ can be obtained through Riccati equation in Eq. (11). The gain vector $\boldsymbol{K}$ can be determined by:

$$\boldsymbol{K}=\begin{bmatrix}2.83\times10^5 & 3.64\times10^4 & 1.45\times10^5 & -1.47\times10^3\end{bmatrix}. \qquad (14)$$

3.3. Disturbance of excitation

The disturbance of excitation on the supporting bearing is caused by various hull deformation, which usually induced by different forces on the ship structure. This disturbance input applied in the control system is obtained through experiments of a shaft platform as shown in Fig. 3, a. The shaft platform is composed of main engine, shaft system, support bearings and propeller.

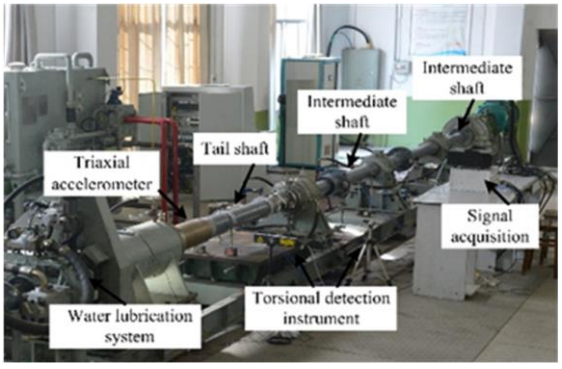

a

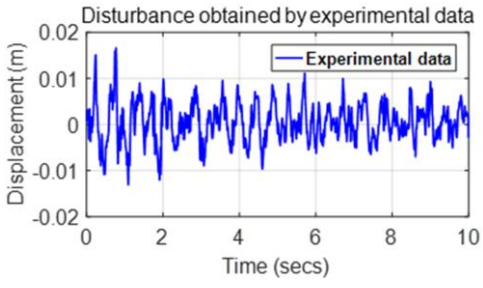

b

Fig. 3 Diagram of shaft experimental platform (a) and the disturbance data obtained by experiment (b)

During the experimental process, the shaft is in a horizontal state and only acted upon by gravity. The torque of the main engine and rotation speed are defined as 184.8 Nm and 100 rpm. The torsional detection instrument (B&K 2523) is installed to test the torque and the rotational speed sensor (B&K MM0024) is placed for the velocity. The triaxial accelerometer sensor (B&K 4535-B-001) is applied for data acquisition of the supporting bearing. The data from 10 seconds of stable operation are selected as the disturbance input to the controlled system. The results in Fig. 3, b displays the transverse response of the bearing with disturbance input. The higher frequency vibration characteristics that may induced by the effect of resistance or damping can be ignored. It can be found that the amplitude of the response is close to 0.0166 m.

4. Results and analysis

The controlled behavior of the active and passive control system will be compared. The behavior specifically includes time response of suspension travel $z_s - z_u$, soleplate deflection $z_u - z_r$, sprung shaft $\ddot{z}_s$ and unsprung bearing $\ddot{z}_u$. Moreover, the robustness analysis is analyzed with a disturbance of pulse width modulation. The influence of the shock absorber damping on the behavior is evaluated and investigated.

4.1. Controlled behavior

The results in Fig. 4 shows the controlled behavior of both the active and passive system. Fig. 4, a indicates the effect of active system in regards to suspension travel $z_s - z_r$, comparing to passive system. The largest displacement is about 0.01 m for the active control, while that of the passive control is close to 0.03 m. It shows an overshoot of about 0.02 m in contrast to the passive control system. Similarly, the it can be seen from Fig. 4, b that the soleplate deflection $z_u - z_r$ of the active system is basically smaller than that of the passive system in general, except for a certain larger value. It can be seen from Fig. 4, c that the acceleration of the sprung shaft $\ddot{z}_s$ with the actuator implemented is superior to that of the passive system. The maximal value of the acceleration in the active system is about -3.53 m/s^2 and it is about -3.69 m/s^2 in the passive system. Similarly, the acceleration of the unsprung bearing $\ddot{z}_u$ in Fig. 4, d also shows noticeable advantages of the active control over the passive control.

The results indicate that the control goal for the marine stern shaft-bearing systems is achieved within a reasonable time interval. The vibration amplitude can be reduced and the irregular movements can be prevented with both active and passive control. And the amplitude is found to be more optimized as the LQR active controller is applied, comparing to that of the passive system.

Fig. 5, a show the displacement comparison of sprung shaft, unsprung bearing and track disturbance in the active system with LQR control implemented. The amplitude of the shaft and bearing is 0.0126 m and 0.0148 m, which is a reduction rate of 24.1% and 10.8% relative to the track disturbance, respectively. Similarly, the comparison of the passive system in Fig. 5, b shows that the maximal value of the shaft is much larger than the track disturbance, while that of the bearing is slightly smaller than the disturbance. The reductions rates are about -100% (0.0332 m) and 22.9%

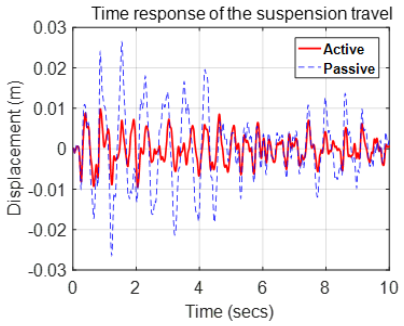

a

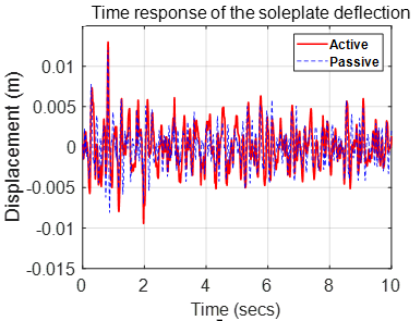

b

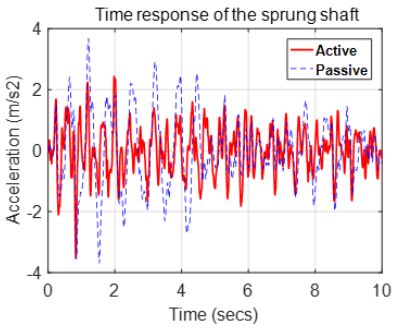

c

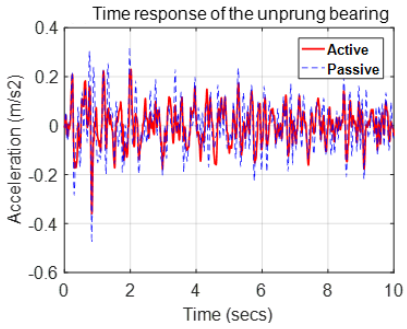

d

Fig. 4 The controlled behavior with active and passive system: a – suspension travel $z_s - z_u$, b – soleplate deflection $z_u - z_r$, c – sprung shaft $\ddot{z}_s$, d – unsprung bearing $\ddot{z}_u$

(0.0128 m), which indicates the shortage of passive system. It can be found that the active system with LQR control is able to reduce the displacement for both sprung shaft and unsprung bearing, comparing to the passive system. Significant improvement is demonstrated in providing more suitable transmission for the shaft.

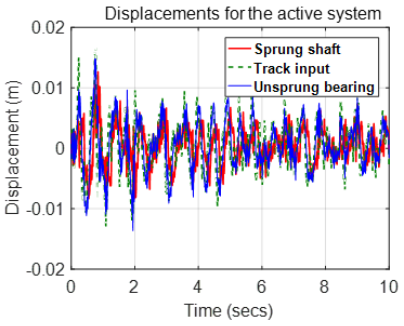

a

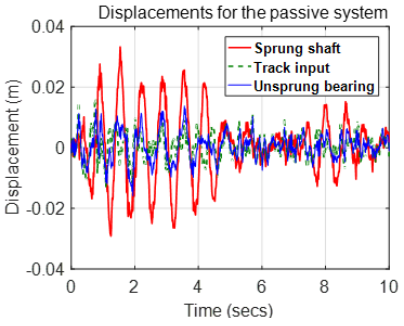

b

Fig. 5 Comparison of the sprung shaft, unsprung bearing and track disturbance: a – active system; b – passive system

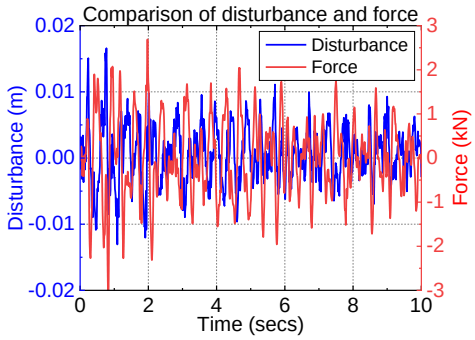

Fig. 6 Comparison of generated force and the disturbance

The advantage of active system is the electromagnetic actuator, which resists undesired vibration of the system. The response in Fig. 6 displays the generated force F_c from the actuator and the disturbance input. It can be seen that the response of the actuator is stable and gives an acceptable response to the disturbance in its original form. The motion of the generated force is in the opposite direction of the disturbance, which can judge the effectiveness of the actuator in active system.

4.2. Robustness of controlled system

The robustness is the ability to reach the control objective in spite of variations in model parameters and disturbance inputs. The changes may be more serious and perhaps unimaginable in actual operation for the insurance of constant stability margin. To study the robustness of the proposal, a disturbance input with a pulse width modulation and attributed to square wave pulses at 6s intervals is applied. The pulse width is 50% of the period with a phase delay of 0.1 s. The amplitude is defined as 0.01 m and the motion

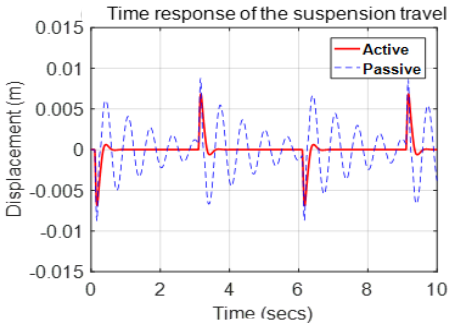

a

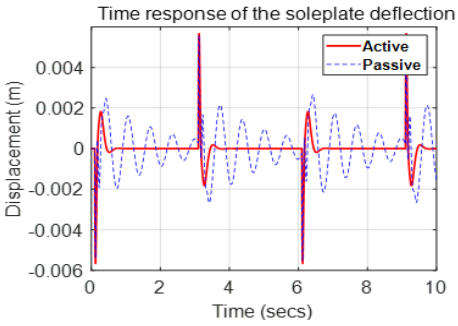

b

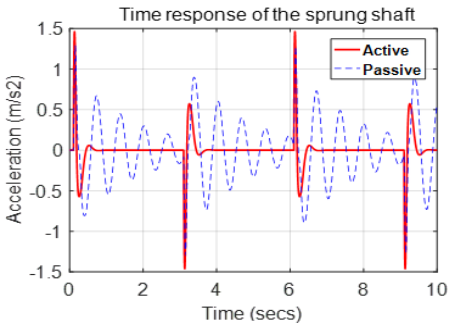

c

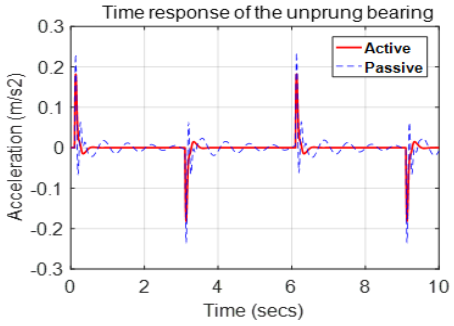

d

Fig. 7 The controlled behavior with active and passive system: a – suspension travel $z_s - z_u$, b – soleplate deflection $z_u - z_r$, c – sprung shaft $\ddot{z}_s$, d – unsprung bearing $\ddot{z}_u$

period is set as 3.0 s.

The displacement of the suspension travel and soleplate deflection, and the acceleration of the sprung shaft and unsprung bearing are shown in Fig. 7. The system experiences oscillations in the period of initial time and then stabilizes gradually to zero in the rest of time. The controlled

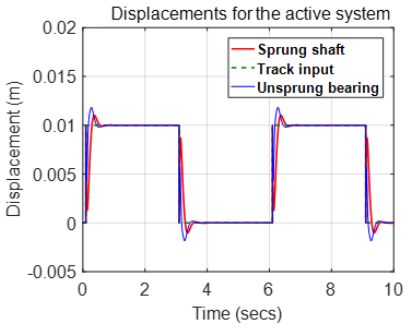

a

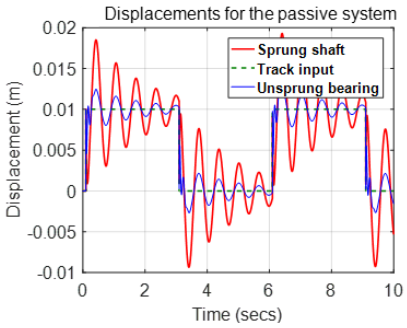

b

Fig. 8 Comparison of the sprung shaft, unsprung bearing and track disturbance: a, active system; b, passive system

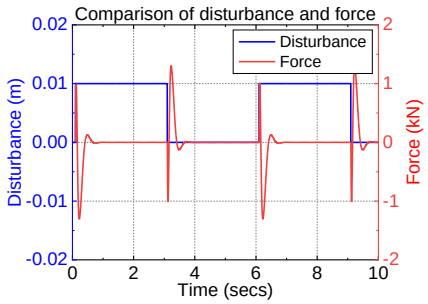

Fig. 9 Comparison of generated force and the disturbance

amplitudes of the active system are found to be optimized, as predicted in Fig. 4. The overshoot with the application of the LQR control is noticed to be about 20% less than that of the passive system, especially for the displacement of suspension travel in Fig. 7, a and the acceleration of bearing in Fig. 7, d. It can be found that the settling time of the active system is significantly shortened, comparing to that of the passive system. The settling time is about 0.8 s with the implement of the LQR control, while it is much hard for the passive system to stabilize over the period of 3 s. It indicates a faster response of the active system to reach stable with more considerable quality.

It can be found in Fig. 8, a that the overshoot rate of the sprung shaft and the unsprung bearing is about 10.1% and 18.2%, respectively. Both the shaft and the bearing of the active system reach steady state in close to the same time frame. The settling time of the shaft has considerably reduced to 0.81s and that of the bearing is about 0.71s. However, Fig. 8, b indicates that the overshoot rate of the passive system improved noticeably, which is about 92.9% and 26.2% for the shaft and bearing.

The force F_c generated by the actuator of the active

system is shown in Fig. 9. It can be noted that the direction of motion is opposite to that of the disturbance input. The direction of the pulse variation is also opposite to the overshoot direction of the active system in Fig. 8, a to ensure the stability of the motion. And the value of the generated force trends to be zero as the system is controlled without fluctuations.

4.3. Influence of the damping

To investigate the influence of adjustable damping shock absorber on the controlled performance, the response of sprung shaft z_s, unsprung bearing z_u and actuator force F_c are selected for the comparison. The damping coefficient of the shock absorber is defined as $c_s * 0.1$, c_s and $c_s * 10$ respectively.

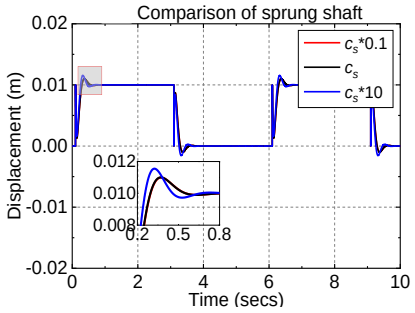

a

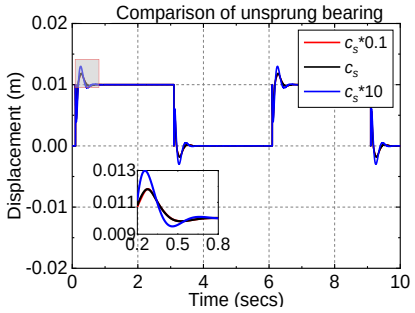

b

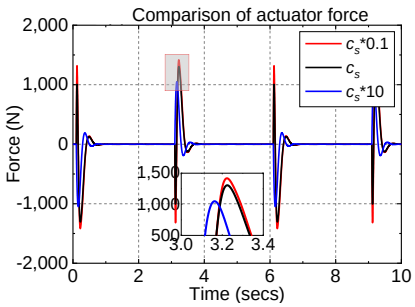

c

Fig. 10 Results comparison with various damping: a – sprung shaft, b – unsprung bearing, c – actuator force

The result in Fig. 10 shows the comparison of controlled behavior with different values of active control damping. It can be seen from Fig. 10, a that the overshoot of the shaft is enlarged with the increase of damping. The overshoot rate for the shaft displacement is 9.9%, 10.1% and 15.5% with the damping ranges from $c_s * 0.1$ to $c_s * 10$. Similarly, the overshoot rate of the bearing is increased by 18.3%, 18.2% and 29.9%, respectively. It indicates that a better controlled behavior of system can be achieved with smaller damping. On the contrary, Fig. 10, c displays the actuator force decreases with increasing damping. The specific values are 1417.8 N, 1305.4 N and 1048.6 N with damping is $c_s * 0.1$, c_s and $c_s * 10$ respectively. This is because of the electromagnetic actuator is applied to resistance the undesired vibration of the system. It needs the largest value for the force to control the displacement of both the shaft and the bearing to be the smallest. The damping can be adjusted to suitable value ranges through the actuator force for better control behavior.

The analysis produces similar results and demonstrate very slight change in the controlled performance with variable damping. Moreover, it shows that the active system with LQR control strategy has good robustness and can adapt to variations of model parameters.

5. Discussion

As the controlled behavior and robustness analysis of the LQR control have been studied. It should be pointed out that the control weighting matrix R has significant influence on the controlled property. To search the suitable value ranges, the controlled behavior with different matrix R are compared. The comparison includes the performance of setting time, overshoot rate and reduction rate. The specific data is listed in the following Table 2.

Table 2
Results comparison of various control weighting matrix R

Parameter	Values	Reduction rate (%)	Overshoot rate (%)	Settling time (s)
R∗0.1	Shaft	28.9	5.3	0.86
	Bearing	8.1	28.1	0.79
R	Shaft	23.8	10.1	1.23
	Bearing	10.9	18.2	1.16
R∗10	Shaft	5.3	32.6	2.40
	Bearing	8.5	16.8	2.31

The reduction rate of the shaft changes from 28.9% to 23.8% and then significantly to 5.3% with increasing control weighting matrix. While, the reduction rate of the bearing increases slightly from 8.1% to 10.9% and then decreases to 8.5%. It demonstrates that the reduction rate of the shaft is more sensitive to the control weighting matrix, especially with larger values of the matrix. While, it is interesting to find that the overshoot rate of the shaft changes gradually from 5.3% to 10.1% and then to 32.6% with the increase of the control weighting matrix. On the contrary, the overshoot rate of the bearing is found to decreases rapidly from 28.1% to 18.2% and then to 16.8%. It gives a choice to define the value of matrix quantitatively according to the control target. It can be noticed that the settling time for both shaft and bearing are enlarged with increased matrix. The settling time for the shaft changes from 0.86 s to 1.23s and then hastily to 2.40 s, and that of the bearing is 0.79 s, 1.23 s and 2.31 s, respectively. It means that the settling time will be more satisfied with smaller control weighting matrix.

As can be seen, the controlled behavior usually remains the performance in spite of changes in the control parameters. The results show that the LQR method performs

better as the control parameters are exactly accurate. Therefore, it is important to adjust the control parameter based on the response to obtain better performance.

6. Conclusions

In this paper, an active LQR control for vibration reduction of the marine stern shaft-bearing system is proposed. The displacement of suspension travel and soleplate deflection, as well as the velocity of shaft and bearing is investigated. The robustness is analyzed with a pulse disturbance to study the maintenance of stability margins. The effect of damping absorber is explored through results discussion with different damping coefficient. The control weighting matrix is proved to be significant for setting time, overshoot rate and reduction rate. Three detailed conclusions can be given:

First, the active control with LQR strategy is applicable for the vibration reduction of the marine stern shaft-bearing systems and is more superior to the passive control. Secondly, the controlled behavior includes reduction rate, overshoot rate and setting time will be more superior with the definition of optimal control parameters. Finally, the controlled behavior of the marine stern shaft-bearing system will be more satisfied with smaller damping and control weighting matrix, especially for the shaft.

In future work, more control strategies will be proposed and compared for the vibration reduction of the marine stern shaft-bearing systems.

Acknowledgments

This research was funded by the National Natural Science Foundation of China (No. 52272377).

References

1. **Zhang, Z.; Duan, N.; Lin, C.; Hua, H.** 2020. Coupled dynamic analysis of a heavily-loaded propulsion shafting system with continuous bearing-shaft friction, International Journal of Mechanical Sciences 172: 105431. https://doi.org/10.1016/j.ijmecsci.2020.105431.
2. **Han, H.; Lee, K.; Jeon, S.; Park, S.** 2017. Lateral-torsional coupled vibration of a propulsion shaft with a diesel engine supported by a resilient mount, Journal of Mechanical Science and Technology 31(8): 3727-3735. https://doi.org/10.1007/s12206-017-0715-y.
3. **Zhang, G.; Zhao Y.; Li, T.; Zhu, X.** 2014. Propeller excitation of longitudinal vibration characteristics of marine propulsion shafting system, Shock and Vibration 2014: 413592. https://doi.org/10.1155/2014/413592.
4. **Murawski, L.** 2012. Some aspects of torsional vibration analysis methods of marine power transmission systems, Journal of Polish CIMAC 7(1): 175-182. Available at: https://api.semanticscholar.org/CorpusID:107168963.
5. **Chahr-Eddine, K.; Yassine, A.** 2014. Forced axial and torsional vibrations of a shaft line using the transfer matrix method related to solution coefficients, Journal of Marine Science and Application 13: 200-205. https://doi.org/10.1007/s11804-014-1251-0.
6. **Sahoo, P.; Chatterjee, S.** 2020. Effect of high-frequency excitation on friction induced vibration caused by the combined action of velocity-weakening and mode-coupling, Journal of Vibration and Control 26(9-10): 735-746. https://doi.org/10.1177/1077546319889866.
7. **Huang, Q.; Shang, T.; Liu, H.** 2023. Harmonic analysis of a marine shaft-bearing suspension system and its semi-active control with PID strategy, Ocean Engineering, 280: 114691. https://doi.org/10.1016/j.oceaneng.2023.114691.
8. **Balaji, P.S.; Karthik SelvaKumar, K.** 2021. Applications of nonlinearity in passive vibration control: a review, Journal of Vibration Engineering & Technologies 9: 183-213. https://doi.org/10.1007/s42417-020-00216-3.
9. **Zhang, G.; Zhao, Y.** 2012. Reduced-order modeling method for longitudinal vibration control of propulsion shafting, Ieri Procedia 1: 73-80. https://doi.org/10.1016/j.ieri.2012.06.013.
10. **Huang, X.; Su, Z.; Hua, H.** 2018. Application of a dynamic vibration absorber with negative stiffness for control of a marine shafting system, Ocean Engineering 155: 131-143. https://doi.org/10.1016/j.oceaneng.2018.02.047.
11. **Jee, J.; Kim, C.; Kim, Y.** 2020. Design improvement of a viscous-spring damper for controlling torsional vibration in a propulsion shafting system with an engine acceleration problem, Journal of Marine Science and Engineering 8(6): 428. https://doi.org/10.3390/jmse8060428.
12. **Liu, G.; Lu, K.; Zou, D.; Xie, Z.; Rao, Z.; Ta, N.** 2017. Development of a semi-active dynamic vibration absorber for longitudinal vibration of propulsion shaft system based on magnetorheological elastomer, Smart Materials and Structures 26(7): 075009. https://doi.org/10.1088/1361-665X/aa73f3.
13. **Zaccardo, V.; Buckner, G.** 2021. Active magnetic dampers for controlling lateral rotor vibration in high-speed rotating shafts, Mechanical Systems and Signal Processing 152: 107445. https://doi.org/10.1016/j.ymssp.2020.107445.
14. **Nath, J.; Chatterjee, S.** 2018. Nonlinear control of stick-slip oscillations by normal force modulation, Journal of Vibration and Control, 24(8): 1427-1439. https://doi.org/10.1177/1077546316661046.
15. **Benassi, L.; Elliott, S.; Gardonio, P.** 2004. Active vibration isolation using an inertial actuator with local force feedback control, Journal of Sound and Vibration 276 (1-2): 157-179. https://doi.org/10.1016/j.jsv.2003.07.019.
16. **Huang, Q.; Xie, Z.; Liu, H.** 2023. Active control for stick-slip behavior of the marine propeller shaft subjected to friction-induced vibration, Ocean Engineering 268: 113302. https://doi.org/10.1016/j.oceaneng.2022.113302.
17. **Zheng, H.; Hu, F.; Qin, H.; Zhang, Z.** 2019. Active control of longitudinal vibration of a tme-varying shafting system with a dynamic interpolating adaptive method, Journal of Vibration and Acoustics – Transactions of the ASME 141(1): 011010. https://doi.org/10.1115/1.4040676.
18. **Xie, X.; Ren, M.; Zhu, Y.; Zhang, Z.** 2020. Simulation and experiment on lateral vibration transmission control of a shafting system with active stern support, International Journal of Mechanical Sciences 170: 105363. https://doi.org/10.1016/j.ijmecsci.2019.105363.

19. **Duan, N.; Wu, C.; Huang, Y.; Zhang, Z.; Hua, H.** 2023. Lateral vibration analysis and active control of the propeller-shafting system using a scaled experimental model, Ocean Engineering 267: 113285. https://doi.org/10.1016/j.oceaneng.2022.113285.
20. **Sinou, J.; Chomette, B.** 2021. Active vibration control and stability analysis of a time-delay system subjected to friction-induced vibration, Journal of Sound and Vibration 500: 116013. https://doi.org/10.1016/j.jsv.2021.116013.
21. **Krama, A.; Gharib, M.; Refaat, S.; Palazzolo, A.** 2021. Design and hardware in-the-loop validation of an effective super-twisting controller for stick-slip suppression in drill-string systems, Journal of Dynamic Systems, Measurement, and Control – Transactions of the ASME 143(11): 111008. https://doi.org/10.1115/1.4051853.
22. **Denimal, E.; Sinou, J.; Nacivet, S.** 2021. Prediction and analysis of quasi-periodic solution for friction-induced vibration of an industrial brake system with the Generalized Modal Amplitude Stability Analysis, Journal of Sound and Vibration 506: 116164. https://doi.org/10.1016/j.jsv.2021.116164.
23. **Huang, Q.; Liu, H.; Ding, Z.** 2022. Impact factors on friction induced vibration of shaft-bearing system considering stick-slip behavior, Marine Structures 84: 103226. https://doi.org/10.1016/j.marstruc.2022.103226.

Q. Huang, Q. Hu, H. Liu

ACTIVE CONTROL FOR TRANSVERSE VIBRATION OF THE MARINE STERN SHAFT-BEARING SYSTEM WITH LQR STRATEGY

S u m m a r y

The vibration control is essential to suppress amplitude and improve efficiency for the marine stern shaft-bearing systems. An active controller for transverse vibration is proposed by a combination of damping absorber and electromagnetic actuator with LQR strategy. The controller is designed with control methods, the parameters are defined based on the system and the disturbance input is obtained from experiments. The displacement of suspension travel and soleplate deflection, as well as the velocity of shaft and bearing is investigated. The robustness is analyzed with a pulse disturbance to study the maintenance of stability margins. The results demonstrated that the controlled behavior of the LQR strategy is preferable to that of the passive control. Moreover, the effect of damping absorber is explored through results discussion with different damping coefficient. The control weighting matrix is proved to be significant for setting time, overshoot rate and reduction rate of the controlled behavior. A smaller damping coefficient and control weighting matrix are demonstrated to be more satisfied for the control objectives. Therefore, the vibration reduction of the marine stern shaft-bearing systems can be achieved with the proposed LQR strategy.

Keywords: active control, transverse vibration, marine shaft-bearing system, LQR strategy, robustness analysis.

Received October 18, 2023
Accepted June 20, 2024